The Astrophysical Journal Supplement Series, 199:11 (6pp), 2012 March doi:10.1088/0067-0049/199/1/11
© 2012. The American Astronomical Society. All rights reserved. Printed in the U.S.A.

VOYAGER OBSERVATIONS OF THE DIFFUSE FAR-ULTRAVIOLET RADIATION FIELD

Jayant Murthy[1], Richard Conn Henry[2], and Jay B. Holberg[3]
[1] Indian Institute of Astrophysics, Bengalooru 560 034, India; jmurthy@yahoo.com
[2] Department of Physics and Astronomy, The Johns Hopkins University, Baltimore, MD 21218, USA
[3] Lunar and Planetary Laboratory, University of Arizona, Tucson, AZ 85721, USA
Received 2011 September 9; accepted 2011 November 29; published 2012 February 29

ABSTRACT

The two *Voyager* spacecraft have completed their planetary exploration mission and are now probing the outer realms of the heliosphere. The *Voyager* ultraviolet spectrometers continued to operate well after the *Voyager 2* Neptune encounter in 1989. We present a complete database of diffuse radiation observations made by both *Voyagers*: a total of 1943 spectra (500–1600 Å) scattered throughout the sky. These include observations of dust-scattered starlight, emission lines from the hot interstellar medium, and a number of locations where no diffuse radiation was detected, with the very low upper limit of about 25 photons cm^{-2} s^{-1} sr^{-1} $Å^{-1}$. Many of these observations were from late in the mission when there was significantly less contribution from interplanetary emission lines and thus less contamination of the interstellar signal.

Key words: surveys – ultraviolet: ISM

Online-only material: color figures, figure set, machine-readable tables

1. INTRODUCTION

The two *Voyager* spacecraft were launched in late 1977 (*Voyager 1* on September 5 and *Voyager 2* on August 20) by the National Aeronautics and Space Administration (NASA) with a mission objective of exploring the giant planets (Kohlhase & Penzo 1977). *Voyager 1* encountered Jupiter and Saturn in 1979 and 1980, respectively, while *Voyager 2* took advantage of a favorable planetary alignment to fly past all four Jovian planets culminating in the Neptune flyby in 1989. The results from the planetary observations revolutionized our understanding of the outer planets and have laid the foundation for many future planetary missions. Less well known are the heliospheric and interstellar observations obtained by both spacecraft while traveling between planetary encounters and continuing until the present date, albeit with reduced capabilities.

Our main interest is in the ultraviolet spectrometers (UVS) carried by each of the two spacecraft (Broadfoot et al. 1977; Holberg & Watkins 1992). These two spectrometers observed various targets between 1977, soon after launch, and well past the 1989 Neptune encounter. Due to declining power from the radioisotope thermoelectric generators (RTG) which powered the spacecraft, the *Voyager 2* UVS was turned off in 1998 and while the *Voyager 1* UVS still continues to transmit data, it can only view a fixed direction in the sky. Many of these observations were of the diffuse far-ultraviolet (FUV: 912–1200 Å) radiation field and all observations until 1994 were compiled by Murthy et al. (1999) with a promise to "process the remainder of the observations in the near future."

Now that UVS observations have been completed (the *Voyager 1* UVS currently only monitors the interplanetary H I Lyα emission) and the spacecraft are close to leaving the solar system, we believe that the time is right to publish the entire UVS set of diffuse observations. There are few instruments capable of observations in the FUV and the *Voyager* UVS were the only ones to undertake a significant number of observations with a sensitivity to the diffuse radiation field of better than 100 photons cm^{-2} s^{-1} sr^{-1} $Å^{-1}$ because of their relatively large field of view. We focus in this work on simply presenting the results and the spectra: a total of 1943 observations spread throughout the sky (Figure 1).

2. OBSERVATIONS AND DATA PROCESSING

The two *Voyager* UVS instruments are identical Wadsworth-mounted objective grating spectrometers covering the spectral range between 500 and 1700 Å over a field of view of $0.^{\circ}1 \times 0.^{\circ}87$. The spectral resolution of each instrument is 38 Å for aperture filling diffuse sources and 18 Å for point sources with a bin size of 9.26 Å. The UVS is most sensitive at wavelengths shortward of 1200 Å with a rapidly declining response at longer wavelengths (Figure 2), where the *Voyager* absolute calibration is based on pre-flight tests at the Kitt Peak vacuum facility and verified by periodic observations of stars (Holberg et al. 1982, 1991). Other than a 30% drop in the sensitivity of the *Voyager 1* UVS during the Jovian encounter, the instrumental calibration remained stable over a period of several years.

A typical *Voyager* sky observation consists of a series of individual accumulations with integration times of commonly either 3.84 s or 576 s, although other integration times were used at different times in the mission, with a total sky exposure for an individual target ranging up to several million seconds. These data were transmitted to Earth where they were picked up by the Deep Space Network antennae and finally sent to the Lunar and Planetary Laboratory of the University of Arizona where they are currently archived.

The archived data are stored as a time-ordered series of spectral records on disk with information about each record contained in a header at the beginning of the record. Murthy et al. (1999) developed a set of routines designed to process these data into a single spectrum for each observation. We have used the same routines, available on request, in this work. The first step in the analysis was to separate the archived data into a set of observations, where an observation is defined as a continuous series of records where the UVS looks at a single region in the sky. The guidance system operates such that the spacecraft executes a slow quasi-random motion about the observation direction of about $0.^{\circ}1$, the width of the slit. If the observed

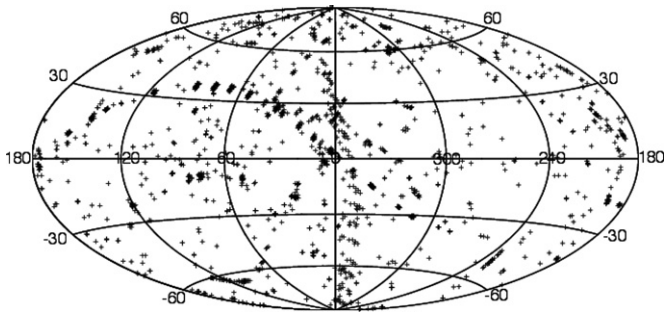

Figure 1. Distribution of *Voyager* observations. The Galactic center is at the origin in this Aitoff plot.

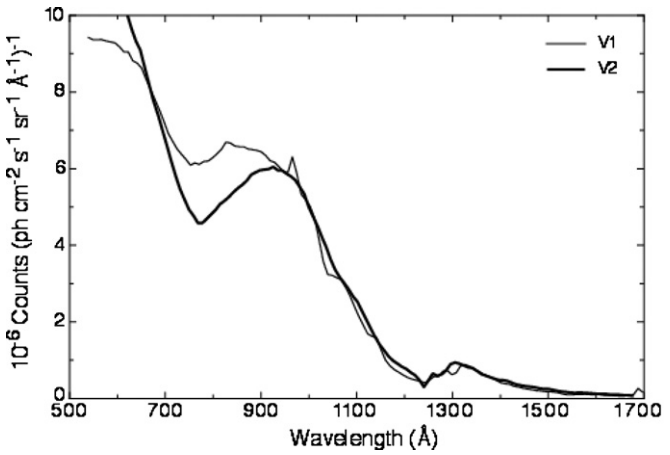

Figure 2. *Voyager 1* and *2* calibration curves. The sensitivity of the UVS instruments is significantly lower at wavelengths longer than 1200 Å.

source is a star (or other point source), the signal will be strongly modulated as the source moves in and out of the field of view, unlike the steady signal from a diffuse source. We used this behavior to reject all point-source observations, leaving us with 1977 potential observations of diffuse radiation of which, as described below, 1943 were usable.

There were two sources of non-astronomical background in these spectra. The first of these was detector noise in the detectors caused by the decay of the plutonium in the RTG. This was measured through periodic observations of a calibration plate on the spacecraft from which no celestial signal could be expected (Table 1). We scaled the RTG spectrum to the observed spectrum below 912 Å (the Lyman limit), with the assumption that there is no astrophysical emission there, and subtracted it. Still remaining were the resonantly scattered heliospheric Lyman lines—Lyα at 1216 Å and Lyβ at 1027 Å.

Murthy et al. (1999) found that the Lyβ/Lyα ratio was constant throughout the mission and that scattering artifacts proportional to the strength of the Lyα line extend throughout the spectrum. This implied that we could choose a single template in which there was no astrophysical emission, scale it to the Lyα line, and subtract it from the data. We sorted through the observations to find the minimum emission in the spectral range from 900 to 1200 Å and assumed that that spectrum defined our effective zero level. While evaluating the spectra, it became apparent that the template itself changed during the mission, particularly after a planetary encounter. Thus, we required three templates in the *Voyager 1* analysis, with a change after each of the two planetary encounters (Table 2). The template was less stable for *Voyager 2* and we required a total of 10 templates

Table 1
Voyager RTG Log

	Year	Exposure Time (s)	Dates Used
		Voyager 1 RTG	
R1	1978.51	259200	1977.70–1979.19
R2	1979.88	163584	1979.20–1980.63
R3	1981.38	365760	1980.63–1983.37
R4	1985.66	628416	1983.73–1986.37
R5	1987.92	523008	1986.88–1989.30
R6	1992.45	417360	1990.58–1992.85
R7	1993.47	257520	1993.43–1994.27
R8	1995.08	182880	1994.27–1995.48
R9	1995.88	660480	1995.48–1996.96
R10	1998.05	357600	1996.97–1999.60
R11	2001.34	61440	1999.77–2001.84
		Voyager 2 RTG	
R12	1978.61	327600	1977.67–1979.45
R13	1980.3	813430	1979.46–1984.59
R14	1984.61	794520	1984.61–1985.50
R15	1986.39	26146.2	1985.50–1987.41
R16	1988.64	902016	1987.85–1988.96
R17	1989.34	44577.2	1989.26–1991.22
R18	1993.26	347238	1991.31–1993.30
R19	1995.12	198000	...
R20	1996.93	246240	...
R21	1997.08	71520	...
R22	1997.55	939360	1993.30–1998.86
R23	1997.72	33120	...

Table 2
Voyager Template Log

	Year	Exposure Time (s)	*L*	*B*	Dates Used
			Voyager 1 Templates		
T1	1977.95	114144	134.2	27.3	1977.70–1978.37
T2	1979.34	142080	115.0	−64.3	1978.61–1993.75
T3	1998.09	303120	143.5	89.3	1993.93–2001.79
			Voyager 2 Templates		
T4	1977.93	308501	109.5	−62.2	1977.92–1978.35
T5	1979.68	65856	103.4	−65.0	1978.81–1980.73
T6	1981.35	98385	70.6	−41.9	1981.03–1981.95
T7	1983.07	249748	74.8	−58.3	1982.35–1984.06
T8	1984.57	40896	173.4	14.6	1984.47–1986.44
T9	1988.43	61170	12.9	47.6	1986.87–1988.96
T10	1989.73	15824	184.9	−59.7	1989.27–1989.75
T11	1992.22	52956	71.4	−29.3	1990.37–1995.20
T12	1996.14	43920	14.4	81.1	1995.42–1996.35
T13	1997.18	250080	62.8	−27.9	1996.55–1997.28
T14	1998.26	50640	4.2	−82.4	1997.28–1998.72

based on the mission date (Table 2). The RTG and template spectra are listed in Table 3 along with the calibration spectra.

Apart from the RTG and template observations, we rejected 20 observations, most of them because of excess emission in the spectral region shortward of 912 Å, perhaps due to a source in the small occultation port. This left a total of 1943 (832 V1 and 1111 V2) observations of the diffuse radiation field with the observation log given in Table 4. Each of the spectra, after subtraction of the RTG induced background and the interplanetary emission, is plotted in Figure 3 and the spectra themselves are tabulated in Table 5 for the *Voyager 1*

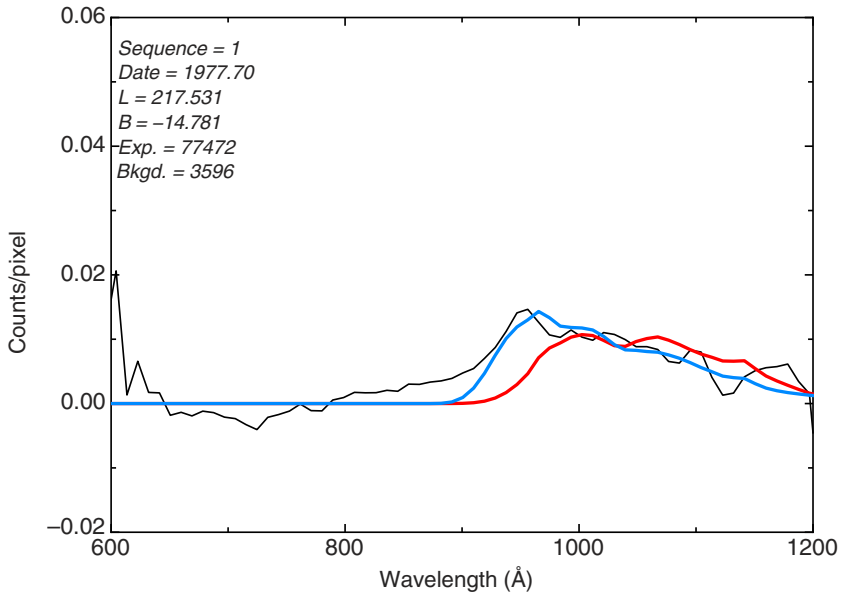

Figure 3. Spectra of *Voyager 1* and *Voyager 2* observations. Overplotted are the best-fit O star template spectra (blue) and B star template spectra (red). The internal sequence number, observation date, galactic coordinates of each target, exposure time, and best-fit B star values are listed in each spectrum.

(A color version and the complete figure set (1943 images) are available in the online journal.)

Table 3
Voyager RTG and Template Spectra

V1 Wavelength (Å)	*V2* Wavelength (Å)	*V1* Calibration	*V2* Calibration	*R*1	*R*2 (counts s^{-1} $pixel^{-1}$)	*R*3	*R*4
539.46	518.08	106122	86827	1.2443	1.1398	1.1300	1.0525
548.72	527.34	106773	86020	1.0569	1.0134	0.9917	0.9645
557.98	536.6	106764	86566	1.8658	1.1177	1.0956	1.9748
567.24	545.86	106755	86711	2.0477	0.9493	0.9385	2.0562
576.5	555.12	107166	88120	1.1813	0.7587	0.7459	0.8202
585.76	564.38	107448	89053	1.1210	0.8016	0.8062	0.6907
595.02	573.64	107740	90376	1.1629	0.8072	0.8164	0.8456
604.28	582.9	108941	91486	1.0872	0.8874	0.9248	0.8799

Notes. The wavelengths for the UVS on the two spacecraft are offset by about 21 Å. The calibration coefficients are in units of photons cm^{-2} s^{-1} sr^{-1} $Å^{-1}$ (counts s^{-1} $pixel^{-1}$)$^{-1}$.

(This table is available in its entirety in a machine-readable form in the online journal. A portion is shown here for guidance regarding its form and content.)

Table 4
Voyager Observation Log

Sequence (1)	S/c (2)	Date (3)	Exposure time (4)	GL (5)	GB (6)	$E(B-V)$ (7)	IR100 (8)	*GALEX* (9)
1	1	1977.7	77472	217.53	−14.78	0.75	16.04	−1
2	1	1977.94	5604	275.29	60.62	0.02	1.02	427
3	1	1978.01	10572	183.69	−17.73	0.48	12.84	3491
4	1	1978.04	37416	328.39	53.09	0.03	1.4	632
5	1	1978.04	33564	120.29	−25.37	0.06	2.66	1122
6	1	1978.01	8292	183.71	−17.7	0.49	13.16	3491

Notes. Column 1: internal sequence number; Column 2: spacecraft (*Voyager 1* or *Voyager 2*); Column 3: mean date of observation; Column 4: total exposure time (s); Column 5: mean galactic longitude of observation; Column 6: mean galactic latitude of observation; Column 7: $E(B-V)$ from Schlegel et al. (1998); Column 8: 100 μm emission (MJy sr^{-1}) from Schlegel et al. (1998); Column 9: *GALEX* FUV (photons cm^{-2} s^{-1} sr^{-1} $Å^{-1}$ at 1517 Å) emission from Murthy et al. (2010).

(This table is available in its entirety in a machine-readable form in the online journal. A portion is shown here for guidance regarding its form and content.)

observations and in Table 6 for *Voyager 2*. There is an extreme range in both exposure time and level of the diffuse flux and, although all the spectra are usable, their quality should be examined before detailed analysis.

3. RESULTS AND DISCUSSION

Most of the diffuse spectra presented in this work are of starlight scattered from interstellar dust and so we have fit each

Table 5
Voyager 1 Spectra

Wavelength	Sequence					
(Å)	1	2	3	4	5	6
539.46	0.0705	0.0035	−0.0233	0.0736	0.0189	−0.0231
548.72	0.0651	0.0017	−0.0221	0.0642	0.0153	−0.0222
557.98	0.0651	0.0017	−0.0221	0.0642	0.0153	−0.0222
567.24	0.1307	0.0066	−0.0114	0.1062	0.0279	−0.0106
576.50	0.1307	0.0066	−0.0114	0.1062	0.0279	−0.0106
585.76	0.0507	0.0376	0.0736	0.0265	0.0040	0.0766
595.02	0.0110	0.0343	0.0792	−0.0049	−0.0027	0.0756

Notes. Sequence references the internal sequence number and may be cross-referenced between tables.

(This table is available in its entirety in a machine-readable form in the online journal. A portion is shown here for guidance regarding its form and content.)

Table 6
Voyager 2 Spectra

Wavelength	Sequence					
(Å)	834	835	836	837	838	839
518.08	0.0039	−0.0291	0.0580	−0.0282	0.0356	−0.0336
527.34	0.0034	−0.0242	0.0472	−0.0234	0.0268	−0.0277
536.60	0.0034	−0.0242	0.0472	−0.0234	0.0268	−0.0277
545.86	0.0009	−0.0183	0.0450	−0.0182	0.0497	−0.0225
555.12	0.0009	−0.0183	0.0450	−0.0182	0.0497	−0.0225
564.38	−0.0118	0.0367	−0.0058	0.0365	0.0513	0.0341
573.64	−0.0226	0.0729	−0.0293	0.0733	0.0613	0.0698

Notes. Sequence references the internal sequence number and may be cross-referenced between tables.

(This table is available in its entirety in a machine-readable form in the online journal. A portion is shown here for guidance regarding its form and content.)

Table 7
Fits to Diffuse *Voyager* Signal

Sequence	Chisq1	Bkgd1	ΔBkgd1	Chisq2	Bkgd2	ΔBkgd2
(1)	(2)	(3)	(4)	(5)	(6)	(7)
1	0.24	2616	200	1.92	3596	300
2	0.89	272	220	0.88	470	340
3	0.93	1206	180	0.61	2040	280
4	1.63	1199	100	3.14	1664	150
5	6.06	1856	80	1.86	3107	120
6	2.17	1454	140	1.05	2524	210
7	8.00	1584	70	1.76	2720	100
8	10.20	1326	50	8.08	2117	70

Notes. Column 1: internal sequence number; Column 2: Chisq for an O star template fit; Column 3: flux of the model fit at 1100 Å Column 4: 1σ error in the model fit; Column 5: Chisq for a B star template fit; Column 6: flux of the model fit at 1100 Å; Column 7: 1σ error in the model fit.

(This table is available in its entirety in a machine-readable form in the online journal. A portion is shown here for guidance regarding its form and content.)

spectrum with both B star and O star templates (plotted in Figure 3) and tabulated the model fits in Table 7. Note that these fits are only for illustrative purposes and do not imply that the radiation in any particular direction is due to dust-scattered starlight. There are also a number of observations of supernovae remnants with strong line emission, primarily from the C III (977 Å) and O VI (1032/1038) lines as observed, for instance, in Vela (Blair et al. 1995). These, and other similar observations, will require follow-up.

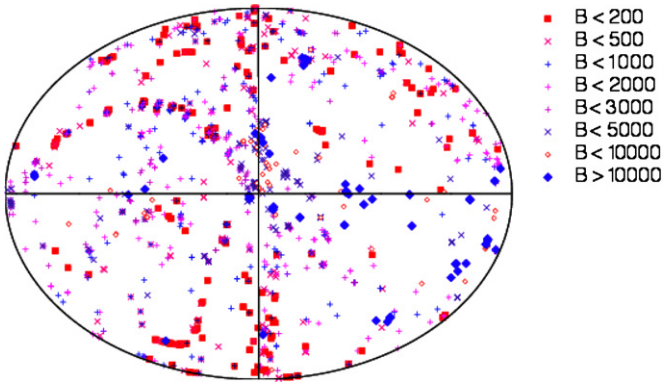

Figure 4. *Voyager* diffuse fluxes in units of photons cm^{-2} s^{-1} sr^{-1} Å^{-1}. The Galactic center is at the origin.

(A color version of this figure is available in the online journal.)

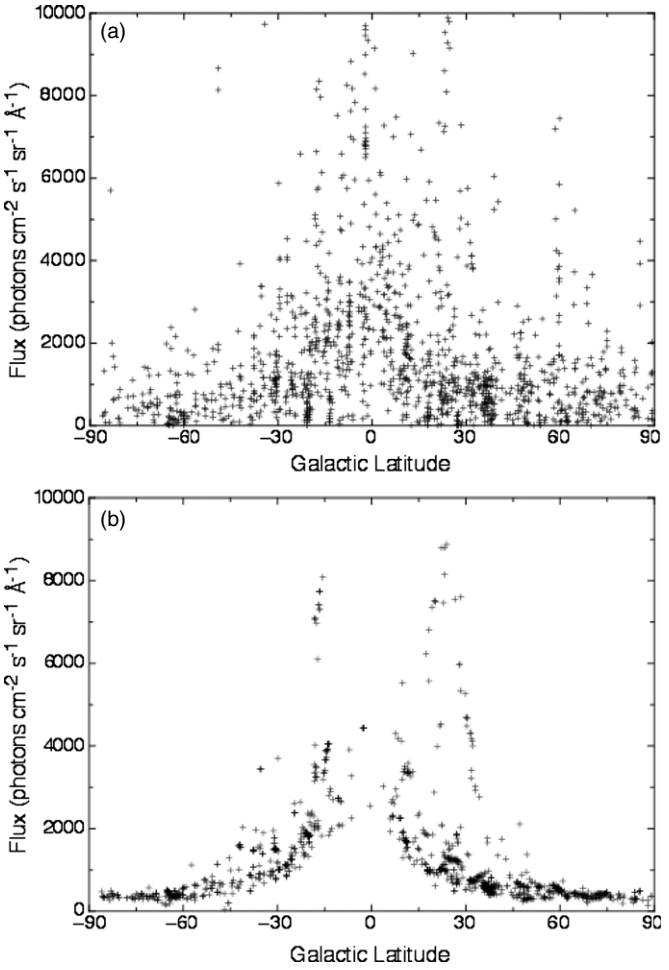

Figure 5. (a) Distribution of the *Voyager* observed brightness with galactic latitude. (b) Distribution of *GALEX* observed brightness with galactic latitude.

In order to study the dust scattered radiation, we used those observations of greater than 10,000 s in exposure time and no obvious interstellar line emission: a total of 1518 observations. The background values at 1100 Å, or rather the best-fit model values at 1100 Å assuming a B star template, are plotted in Figure 4, highlighting both the faintest observations (<200 photons cm^{-2} s^{-1} sr^{-1} Å^{-1}) and the brightest (>10,000 photons cm^{-2} s^{-1} sr^{-1} Å^{-1}). Although the overall distribution of the diffuse background follows a cosecant law falling off from the Galactic plane (Figure 5(a)), it is

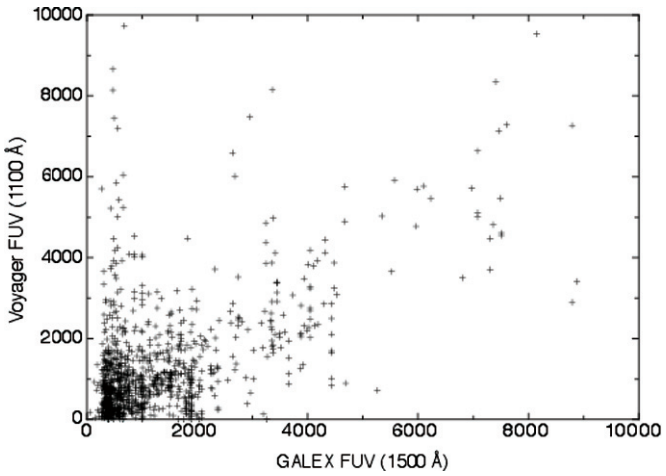

Figure 6. Correlation between *Voyager* and *GALEX* observed backgrounds.

Table 8
Voyager 1 Zero Levels

Sequence (1)	Date (2)	Gal. Long. (3)	Gal. Lat. (4)	Exp. Time (5)	Flux (6)	*GALEX* FUV (7)
192	1981.42	35.9	27.6	365760	-4 ± 10	1137
248	1992.47	314.8	20.9	450480	10 ± 15	...
316	1995.09	316.2	27.3	182880	11 ± 15	1756

Notes. Column 1: internal sequence number; Column 2: observation date; Column 3: galactic longitude of observation; Column 4: galactic latitude of observation; Column 5: exposure time; Column 6: flux (photons cm^{-2} s^{-1} sr^{-1} Å^{-1}) at 1100 Å with 1σ error bars; Column 7: *GALEX* FUV flux at 1500 Å (photons cm^{-2} s^{-1} sr^{-1} Å^{-1}).

not as sharply defined as the equivalent distribution at 1500 Å (Figure 5(b)), where we have plotted the values from the all-sky map of the diffuse background observed by the *Galaxy Evolution Explorer* (*GALEX*) satellite (Murthy et al. 2010).

As mentioned above, the dominant source of emission in both wavelength bands is likely to be dust-scattered radiation, in which case the *Voyager* observations should be correlated with the *GALEX* observations. In fact, the correlation between the two is poor (Figure 6) with a correlation coefficient of 0.55, primarily because there are a number of locations at low galactic latitudes where *Voyager* observes little emission but *GALEX* observes significant emission. The converse is also true; there are a number of regions with intense emission in the *Voyager* observations but much less in *GALEX*. The optical depth of the dust grains at 1100 Å is about 40% more than at 1500 Å and thus the diffuse background at 1100 Å is due more to local effects than that at longer wavelengths but this is unlikely to be the source of much of the discrepancy. Other sources of emission include line emission from C III (977 Å) and O VI (1035 Å) in the *Voyager* spectral range (Murthy et al. 1993) and C IV (1550 Å) in the *GALEX* range, and Lyman and Werner band emission from molecular hydrogen contributing to both. A detailed study of the individual regions is needed to understand the diffuse flux in each region.

Observations of the faintest regions in the sky provide information about the systemic errors in our procedure as well as placing strong limits on the level of the diffuse background. To this end, we have identified the three observations (all from *Voyager 1*) which gave the lowest limits on the diffuse background (Table 8) and plotted them in Figure 7 with a B star spectrum scaled to 100 photons cm^{-2} s^{-1} sr^{-1} Å^{-1} at 1100 Å.

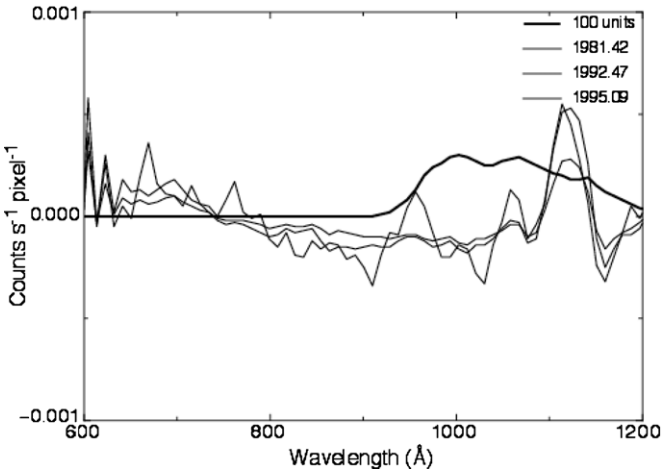

Figure 7. *Voyager 1* spectra of three regions with no observed flux. Overplotted (dark line) is a B star template with a flux of 100 photons cm^{-2} s^{-1} sr^{-1} Å^{-1} at 1100 Å.

These three spectra, after subtraction of the RTG spectrum and the Lyα template, are remarkably consistent despite a 14 year spread in observation date. The observations are all at moderate galactic latitudes and are widely separated in the sky yet show no sign of diffuse radiation, with an upper limit of about 25 photons cm^{-2} s^{-1} sr^{-1} Å^{-1}. *GALEX* observations in the two of these regions find a flux of 1000–2000 photons cm^{-2} s^{-1} sr^{-1} Å^{-1} as expected from models of dust scattering (Draine 2003). Further modeling is required to understand why no signal is observed in the *Voyager* bands.

At the other end of the scale are the bright *Voyager* regions, many of which are at low Galactic latitudes and hence are likely due to starlight scattered from dust in the Galactic disk, while others are observations in the LMC where there are many bright stars and considerable diffuse FUV emission (Pradhan et al. 2010). The dust scattered radiation is patchy in the ultraviolet where the level of scattering depends on the relatively geometry between the dust and those few stars hot enough to contribute photons at these wavelengths and a more detailed study of the individual regions is required to model them.

4. CONCLUSIONS

We have reduced all the diffuse observations made by the two *Voyager* spacecraft from their launch in 1977 to their final UVS observations in 2001 and 1998 for *Voyagers 1* and *2*, respectively: a grand total of 1943 individual pointings. Most of these observations are likely to be of starlight scattered by interstellar dust but there are puzzling contradictions in that there is a poor correlation with the *GALEX* observations at 1500 Å with low *Voyager* fluxes even near the Galactic plane. Other observations show strong emission lines from hot gas, primarily C III (977 Å) and O VI (1035 Å).

We have now amassed a number of observations in different wavelength regimes: the *Voyager* spectra presented here (912–1200 Å); the *GALEX* observations of Murthy et al. (2010) in the FUV (1500 Å); the recent reanalysis of the *Pioneer 10/11* Imaging Photopolarimeter data by Matsuoka et al. (2011) in the visible (4400 Å and 6400 Å); and the infrared data from *IRAS* and the *Cosmic Orbiting Background Explorer* satellites (e.g., Odegard et al. 2007). We plan to integrate these into a model for the diffuse radiation in our Galaxy.

We are grateful to NASA for their wisdom in allowing the *Voyager* spacecraft to continue to make observations long after the end of the planetary mission. This work was partially supported by NASA's Maryland Space Grant Consortium.

REFERENCES

Blair, W. P., Vancura, O., & Long, K. S. 1995, AJ, 110, 312
Broadfoot, A. L., Sandel, B. R., Shemansky, D. E., et al. 1977, Space Sci. Rev., 21, 183
Draine, B. T. 2003, ARA&A, 41, 241
Holberg, J. B., Carone, T. E., & Polidan, R. S. 1991, Adv. Space Res., 11, 33
Holberg, J. B., Forrester, W. T., Shemansky, D. E., & Barry, D. C. 1982, ApJ, 257, 656
Holberg, J. B., & Watkins, R. 1992, Voyager Ultraviolet Spectrometer Guest Observer and Data Analysis Handbook, Version 1.1
Kohlhase, C. E., & Penzo, P. A. 1977, Space Sci. Rev., 21, 77
Matsuoka, Y., Ienaka, N., Kawara, K., & Oyabu, S. 2011, ApJ, 736, 119
Murthy, J., Hall, D. T., Earl, M. E., Henry, R. C., & Holberg, J. B. 1999, ApJ, 522, 904
Murthy, J., Henry, R. C., & Sujatha, N. V. 2010, ApJ, 724, 1389
Murthy, J., Im, M., Henry, R. C., & Holberg, J. B. 1993, ApJ, 419, 739
Odegard, N., Arend, R. G., Dwek, E., et al. 2007, ApJ, 667, 11
Pradhan, A. C., Pathak, A., & Murthy, J. 2010, ApJ, 718, L141
Schlegel, D. J., Finkbeiner, D. P., & Davis, M. 1998, ApJ, 500, 525